

Enhancing Adversarial Transferability via Information Bottleneck Constraints

Biqing Qi^{1,2,3}, Junqi Gao⁴, Jianxing Liu¹, *Senior Member, IEEE*, Ligang Wu¹, *Fellow, IEEE*, Bowen Zhou^{1,2}
Fellow, IEEE

Abstract—From the perspective of information bottleneck (IB) theory, we propose a novel framework for performing black-box transferable adversarial attacks named IBTA, which leverages advancements in invariant features. Intuitively, diminishing the reliance of adversarial perturbations on the original data, under equivalent attack performance constraints, encourages a greater reliance on invariant features that contributes most to classification, thereby enhancing the transferability of adversarial attacks. Building on this motivation, we redefine the optimization of transferable attacks using a novel theoretical framework that centers around IB. Specifically, to overcome the challenge of unoptimizable mutual information, we propose a simple and efficient mutual information lower bound (MILB) for approximating computation. Moreover, to quantitatively evaluate mutual information, we utilize the Mutual Information Neural Estimator (MINE) to perform a thorough analysis. Our experiments on the ImageNet dataset well demonstrate the efficiency and scalability of IBTA and derived MILB. Our code is available at github.com/IBTA.

Index Terms—Adversarial Transferability, Adversarial Attack, Information Bottleneck

I. Introduction

DEEP learning-based models are susceptible to imperceptible adversarial examples (AEs) [1], which often exhibit successful transfer across different models [2], [3], [4], [5]. This characteristic provides a practical advantage in black-box scenarios, where the parameters and structure of the victim model remain unknown. Studying transferable attacks contributes to a deeper comprehension of adversarial vulnerabilities and can offer valuable insights for the development of defense strategies. However, traditional black-box attacks demonstrate limited performance in terms of transferability [3], [6], [7]. Nowadays, various studies delved into transfer attacks and proposed strategies aimed at enhancing the transferability of adversarial attacks. The mainly works can be classified according to their objectives as either targeted or non-targeted attacks. Targeted attacks aim at a specific class, while non-targeted attacks aim to disrupt any class except the original one. In the non-target scenario, numerous strategies involve the incorporation of momentum in the iterative process [8], [9], the utilization of data augmentation [10], [11], and the application

of mixup techniques [12]. Actually, transferring targeted adversarial perturbations poses greater challenges compared to non-targeted settings [13], [14], prompting subsequent research endeavors dedicated to investigating the transferability of targeted attacks. These efforts encompass the use of GAN-generated adversarial perturbations [15], the harnessing of local and global information to enhance contrast [16], the incorporation of 3D transformations [17] into attack strategies, the utilization of spectral transformations, and the formulation of the iterative process as a min-max bi-level optimization problem. Despite extensive research, non-targeted and targeted investigations remain separate. Therefore, a unified perspective for comprehending adversarial transferability is still absent.

To response the above challenge, we introduce a novel perspective for enhancing transferability in adversarial attacks, leveraging the principles of information bottleneck (IB) theory [18], [19]. Our contributions are three-fold. **Firstly**, We are the first to introduce a simple and efficient framework to enhance transferability within adversarial attacks from the information bottleneck perspective. This framework originates from the motivation to diminish correlation on noisy and extraneous features present in the original inputs, thereby improving the transferability of adversarial perturbations. It is formulated by mutual information (MI) techniques. To the best of our knowledge, this conceptual perspective remains unexplored in previous studies. **Secondly**, because direct optimization of the MI between perturbations and the original input is unfeasible, inspired from key ideas in variational inference [20], [21], we derived a lower bound for this measure. Following that, we introduce an efficient loss function known as the IB based transferable loss to facilitate the suppression of MI. **Thirdly**, to quantitatively assess the lower bound of MI, we employed the Mutual Neural Estimator (MINE) technique [22]. We conducted experimental validation to ascertain the effectiveness of our method in suppressing MI. By conducting experiments on the ImageNet dataset, we illustrate that our method consistently enhances performance across various baselines.

A. Motivation

In the context of deep learning models, a fundamental question arises: how do we extract meaningful features from the original data? These features have a significant impact on the model's performance. Inspired by prior works [18], [19], we recognize that invariant features are closely aligned with class information, while non-invariant features consist of noise and instability. Intuitively, invariant features that capture essential information are more versatile, thus enhancing transferability.

¹Department of Control Science and Engineering, Harbin Institute of Technology, Harbin 150001, P. R. China; ² Tsinghua University, Beijing, P. R. China; ³Frontis.AI, Beijing, P. R. China; ⁴School of Mathematics, Harbin Institute of Technology, Harbin 150001, P. R. China; (Email: qibiqing7@gmail.com; gjunqi97@gmail.com; jx.liu@hit.edu.cn; ligangwu@hit.edu.cn; zhoubowen@tsinghua.edu.cn). This work was supported in part by the National Science and Technology Major Project (No. 20232D0121403). *Corresponding authors: Bowen Zhou and Ligang Wu.*

This naturally leads us to inquire: **Can emphasizing the correlation between attacks and invariant features enhance adversarial transferability?** This proposition suggests that if adversarial perturbations primarily depend on invariant features while reducing reliance on non-invariant features and noise in the original data, they will demonstrate superior transferability across a diverse range of models. To achieve this, we apply the IB Theory, which entails a dual purpose: maximizing information extraction from the encoded hidden layer variable denoted as Z with a specific emphasis on the included label Y while ensuring task completion. Simultaneously, we aim to minimize the information related to the input variable X within Z , which can be accomplished by minimizing $I(X; Z) - \beta I(Y; Z)$.

B. Problem Formulation

Formally, in line with the aforementioned motivation, we proceed to reformulate adversarial attacks with the help of IB concepts. With the scope of adversarial attacks, consider a clean sample $(x, y) \in \Omega$, where $\Omega = \mathcal{X} \times \mathcal{Y}$ represents the sample space, and the source model $\mathcal{M}^S(\cdot, \theta)$ is parameterized by $\theta \in \Theta$. We can redefine an adversarial attack as follows:

$$\underset{\|\epsilon\| \leq r}{\text{minimize}} \quad \zeta_{tar} \mathcal{L}_{cls}(\mathcal{M}^S(x + \epsilon, \theta), y_{adv}) + I(\mathcal{E}; X|Y_{adv}), \quad (1)$$

in which r denotes the constraint threshold for the adversarial perturbation, and \mathcal{E} represents the random variable associated with this perturbation. The variable ζ_{tar} takes the value 1 in the target setting and -1 otherwise, while \mathcal{L}_{cls} signifies the classification loss. y_{adv} indicates the label employed during the attack. In the targeted scenario, y_{adv} corresponds to the target class label y_{target} ; otherwise, it defaults to the label y .

C. IB induced Transferable Attacks (IBTA)

Given the optimization objective in Eq. (1), direct optimization of $I(\mathcal{E}; X|Y_{adv})$ is infeasible. To address this challenge, we derive a simple lower-bound to realize approximate computation. Firstly, we consider the information flow during the attack process: $X \rightarrow \mathcal{E} \rightarrow X_{adv} \rightarrow Z_{adv}^\theta$, suppose it forms a Markov chain. Since $z_{adv}^\theta = \mathcal{M}^S(x_{adv}, \theta)$ (Adversarial perturbation z_{adv} in the source side can be easily guaranteed), the information flow becomes $X \rightarrow \mathcal{E} \rightarrow Z_{adv}^\theta$. Expanding MI in two distinct ways:

$$\begin{aligned} I(X; \mathcal{E}, Z_{adv}^\theta | Y_{adv}) &= I(X; Z_{adv}^\theta | Y_{adv}) + I(X; \mathcal{E} | Y_{adv}, Z_{adv}^\theta) \\ I(X; \mathcal{E}, Z_{adv}^\theta | Y_{adv}) &= I(X; \mathcal{E} | Y_{adv}) + I(X; \mathcal{E} | Y_{adv}, Z_{adv}^\theta). \end{aligned} \quad (2)$$

Markovity implies that X and Z_{adv}^θ are conditionally independent given \mathcal{E} , thus $I(X; Z_{adv}^\theta | Y_{adv}, \mathcal{E}) = 0$. Due to the non-negativity of MI, we have:

$$I(X, \mathcal{E} | Y_{adv}) \geq I(X, Z_{adv}^\theta | Y_{adv}). \quad (3)$$

Note that:

$$\begin{aligned} &I(X, Z_{adv}^\theta | Y_{adv}) \\ &= \int p(z_{adv}^\theta, \mathbf{x}, y_{adv}) \log \frac{p(z_{adv}^\theta | \mathbf{x}, y_{adv})}{p(z_{adv}^\theta | y_{adv})} dz_{adv}^\theta dy_{adv} d\mathbf{x} \\ &= \mathbb{E}_{X, Y_{adv}} [\mathcal{D}_{\text{KL}}(p(z_{adv}^\theta | \mathbf{x}, y_{adv}) || p(z_{adv}^\theta | y_{adv}))]. \end{aligned} \quad (4)$$

Algorithm 1 Procedure of IBTA

Require: Surrogate model $\mathcal{M}_S(\cdot, \theta)$, total steps T , step size α , clean input \mathbf{x} , label used for attack y_{adv} , ℓ_∞ perturbation budget r .

- 1: Randomly sample $\boldsymbol{\eta} \leftarrow \mathcal{N}(0, \sigma^2 \mathbf{I})$, $\tilde{\mathbf{x}} \leftarrow \mathbf{x} + \boldsymbol{\eta}$
 - 2: Initialize $\boldsymbol{\epsilon}_0 = 0$, $\mathbf{x}_{adv} \leftarrow \mathbf{x} + \boldsymbol{\epsilon}_0$, $\tilde{\mathbf{x}}_{adv} \leftarrow \Pi_{(0,1)}(\tilde{\mathbf{x}} + \boldsymbol{\epsilon}_0)$
 - 3: **for** $t = 1 \leftarrow T$ **do**
 - 4: $g_t = \nabla_{\boldsymbol{\epsilon}} \mathcal{L}_{IBTA}(\mathbf{z}_{adv}, \tilde{\mathbf{z}}_{adv}, y_{adv})$.
 - 5: $\boldsymbol{\epsilon}_t = \Pi_{(-r,r)}(\boldsymbol{\epsilon}_{t-1} - \alpha * \text{sign}(g_t))$
 - 6: $\mathbf{x}_{adv} = \Pi_{(0,1)}(\mathbf{x} + \boldsymbol{\epsilon}_t)$, $\tilde{\mathbf{x}}_{adv} = \Pi_{(0,1)}(\tilde{\mathbf{x}} + \boldsymbol{\epsilon}_t)$
 - 7: **end for**
 - 8: **return** \mathbf{x}_{adv}
-

We can minimize the lower bound of $I(X, \mathcal{E} | Y_{adv})$ by minimizing $\mathcal{D}_{\text{KL}}(p(z_{adv}^\theta | \mathbf{x}, y_{adv}) || p(z_{adv}^\theta | y_{adv}))$ for all $\mathbf{x} \in \mathcal{X}$, which means we aim to make $p(z_{adv}^\theta | \mathbf{x}, y_{adv})$ as close as possible to $p(z_{adv}^\theta | y_{adv})$ for all $\mathbf{x} \in \mathcal{X}$. According to the definition of marginal distribution, we have

$$\begin{aligned} p(z_{adv}^\theta | y_{adv}) &= \int p(z_{adv}^\theta, \mathbf{x} | y_{adv}) d\mathbf{x} \\ &= \int p(z_{adv}^\theta | \mathbf{x}, y_{adv}) p(\mathbf{x} | y_{adv}) d\mathbf{x} \\ &= \int p(z_{adv}^\theta | \mathbf{x}, y_{adv}) p(\mathbf{x}) d\mathbf{x} \\ &= \mathbb{E}_X [p(z_{adv}^\theta | \mathbf{x}, y_{adv})]. \end{aligned} \quad (5)$$

Therefore, our goal becomes to make $p(z_{adv}^\theta | \mathbf{x}, y_{adv})$ as close as possible to $\mathbb{E}_X [p(z_{adv}^\theta | \mathbf{x}, y_{adv})]$. We can achieve this by reducing the variability of $p(z_{adv}^\theta | \mathbf{x}, y_{adv})$ with respect to \mathbf{x} . In other words, we need that $p(z_{adv}^\theta | \mathbf{x}, y_{adv})$ and $p(\tilde{z}_{adv}^\theta | \tilde{\mathbf{x}}, y_{adv})$ are as close as possible for different $\mathbf{x}, \tilde{\mathbf{x}} \in \mathcal{X}$. To achieve this, we introduce a tiny displacement $\boldsymbol{\eta}$ to \mathbf{x} to simulate $\tilde{\mathbf{x}}$, where $\boldsymbol{\eta} \sim \mathcal{N}(0, \sigma^2 \mathbf{I})$ and σ is a hyperparameter with a small value, aiming to ensure that $\mathbf{x} + \boldsymbol{\eta}$ closely approximates the distribution $p(\mathbf{x})$. Following this, we can introduce the IB induced Loss as depicted below, to help reduce $I(X, Z_{adv}^\theta | Y_{adv})$:

$$\begin{aligned} &\mathcal{L}_{IBTA}(z_{adv}^\theta, \tilde{z}_{adv}^\theta, y_{adv}) \\ &= \mathcal{L}(z_{adv}^\theta, \tilde{z}_{adv}^\theta, y_{adv}) + \gamma \mathcal{L}(\tilde{z}_{adv}^\theta, z_{adv}^\theta, y_{adv}), \end{aligned} \quad (6)$$

and

$$\begin{aligned} &\mathcal{L}(z_{adv}^\theta, \tilde{z}_{adv}^\theta, y_{adv}) = \delta_{tar} \mathcal{L}_{cls}(z_{adv}^\theta, y_{adv}) \\ &\quad + \lambda [\mathcal{D}_{\text{KL}}(p(z_{adv}^\theta | \mathbf{x}, y_{adv}) || p(\tilde{z}_{adv}^\theta | \tilde{\mathbf{x}}, y_{adv}))], \end{aligned} \quad (7)$$

where γ and λ are hyperparameters and $\text{blue } z_{adv}^\theta = \mathcal{M}_S(\mathbf{x} + \boldsymbol{\epsilon}, \theta)$ and $\text{blue } \tilde{z}_{adv}^\theta = \mathcal{M}_S(\tilde{\mathbf{x}} + \boldsymbol{\epsilon}, \theta)$, the classification loss \mathcal{L}_{cls} is used to iteratively compute $\boldsymbol{\epsilon}$. The KL divergence is employed to ensure the proximity between $p(z_{adv}^\theta | \mathbf{x}, y_{adv})$ and $p(\tilde{z}_{adv}^\theta | \tilde{\mathbf{x}}, y_{adv})$. Based on this, we introduce the **IB induced Transferable Attack** (IBTA), its framework is summarized as Algorithm 1. The notation $\Pi_{(a,b)}(\cdot)$ denotes the operation of clipping each element's value to fall within the range (a, b) .

II. Analysis and Experiments

A. Analysis of MI

Impact of $I(\mathcal{E}; X | Y_{adv})$. To quantitatively evaluate the efficiency of our framework for reducing $I(\mathcal{E}; X | Y_{adv})$, we

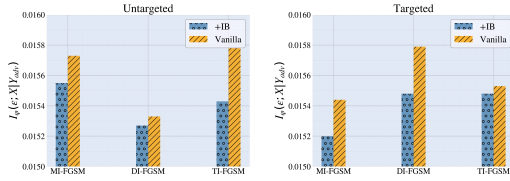


Fig. 1. The values of computed $I_\varphi(\mathcal{E}; X|Y_{adv})$ under targeted and non-targeted settings, with “+IBTA” indicating the addition of IBTA during the iteration process.

employed the MINE technique [22] with the help of an M -bounded estimator T_φ parameterized by φ to compute $I_\varphi(\mathcal{E}; X|Y_{adv})$, i.e. $e^{T_\varphi}, T_\varphi \leq M$. $\varphi \in \Phi \subset \mathbb{R}^d$, $\|\varphi\| \leq K$, and T_φ is L -Lipschitz. As the training sample size n increases, the estimated $I_\varphi(\mathcal{E}; X|Y_{adv})$ will method the true $I(\mathcal{E}; X|Y_{adv})$ from below, which is ensured by Theorem 1.

Theorem 1: (Theorem 3 in [22]) Given any values ξ , δ of the desired accuracy and confidence parameters, we have

$$\Pr(|\widehat{I(X; Z)}_n - I_\Theta(X, Z)| \leq \xi) \geq 1 - \delta, \quad (8)$$

whenever the number n of samples satisfies

$$n \geq \frac{2M^2(d \log(16KL\sqrt{d}/\xi) + 2dM + \log(2/\delta))}{\xi^2}. \quad (9)$$

In our experiments, we conducted a random selection of ten classes (31, 56, 241, 335, 458, 532, 712, 766, 887, 975) from the ImageNet dataset [23] for training purposes. The estimator was trained using the respective training dataset, and adversarial perturbations were computed for this training data. Experiments were performed in both targeted and non-targeted settings using three classical baseline attack methods: MIM [8], DIM [11], and TIM [10]. The values of λ , γ , and σ were set to 0.01, 0.1, and 0.1 respectively. We employed ResNet50 (Res50) [24] as our source model. The perturbation budget was defined as $r = 16$, with $\alpha = 2$ and $T = 20$. The experimental results, as depicted in Figure 2, illustrate the effectiveness of our method in reducing $I(\mathcal{E}; X|Y_{adv})$.

Impact of hyperparameters. To investigate the impact of various hyperparameter choices on our method, we conducted comparative experiments using the MIM+IBTA method with different hyperparameter magnitudes. The source model employed was ResNet50 (Res50), while the target models evaluated included ResNet152 (Res152) [24], DenseNet121 (Dense121) [25], and VGG19bn [26]. We calculated the average transfer success rate across these three models. All other experimental settings remained consistent with those detailed in Section III.A. The results are presented in Figures 3 and 4. When σ was set to 1, a decrease in transferability was observed in both target and non-targeted scenarios, with a more significant reduction in the non-targeted scenario. This phenomenon stems from the substantial deviation of $x + \eta$ from the original distribution $p(x)$ when sigma is excessively large. In non-targeted scenarios, choosing a larger λ often resulted in a lower transfer success rate. This is because, in targeted scenarios, it suffices to include as much information about the target class as possible in ϵ . However, in non-targeted scenarios, we need to perturb x and \tilde{x} in directions that maximize their original class classification losses, which are likely to be inconsistent. A larger lambda exacerbates this imbalance.

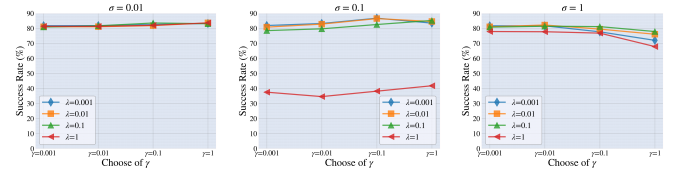


Fig. 2. Transfer success rates of MIM+IBTA with different parameter settings in the untargeted scenario.

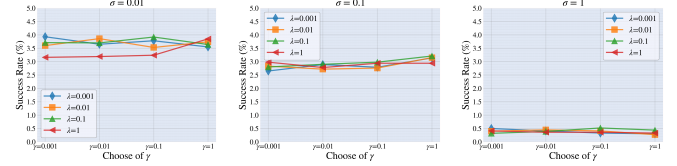


Fig. 3. Transfer success rates of MIM+IBTA with different parameter settings in the targeted scenario.

In non-targeted settings with $\sigma = 1$, increasing gamma led to some performance degradation, whereas in targeted settings with $\sigma = 0.01$, it yielded a certain degree of improvement. For stability, we opted for $\lambda = 0.1$, $\sigma = 0.1$, and $\gamma = 0.1$ in subsequent experiments.

B. Analysis of Expandability

In this section, we explore the expandability of IBTA as a general framework for seamless integration into existing attack methods. We selected MIM, DIM, and TIM as baselines. Following the same settings as in Section III-A, we conducted experiments using the randomly selected ImageNet subset. The images were first resized to 256×256 and then center-cropped to 224×224 . The momentum factor μ for MIM was set to 0.1, the probability p for input diversity in DIM was set to 0.7, and the kernel length for TIM was set to 7. The experiments are under multiple step-size settings in both targeted and non-targeted scenarios. For targeted attacks, we used three different step sizes: 20, 100, and 300. For non-targeted attacks, we used three step sizes: 20, 40, and 60. Following [14], we use Res50, Res152, Dense121, and VGG19bn as source models sequentially and test the transfer success rate on the remaining three models. The results are presented in Table I. Our method demonstrates improvement in both targeted and non-targeted settings, especially in the targeted setting where it achieves a maximum improvement of 6.07%. In the non-target setting, where DIM and TIM already perform well, our method still provides efficient improvement. Meanwhile, on the source model VGG19bn, where the vanilla methods are not so strong, our method still achieves an average improvement of over 4%. This confirms the effectiveness of our framework in transfer attacks and demonstrates the expandability of our framework with other existing methods.

C. Comprehensive Experiments

Following [27], we conducted experiments on several additional models. We selected Inception-v3 (Inc-v3) [28] and an ensemble model composed of three models (Res152, Dense121, and Inc-v3) as the source models. As for the target models, we chose Inception-v4 (Inc-v4) [29], Inception-ResNet-v2 (IncRes-

TABLE I

TRANSFER SUCCESS RATE (%) FOR TRANSFERABLE ATTACKS, WHERE THE VALUES IN THE TABLE REPRESENT THE RESULTS OF 20/40/60 ATTACK STEPS.

Attack	Src:Res50 (untargeted)					Src:Dense121 (untargeted)				
	→Res50*	→VGG19bn	→Dense121	→Res152	AVG Transfer Rate	→Dense121*	→VGG19bn	→Res152	AVG Transfer Rate	
MIM	100.00/100.00/100.00	78.20/76.20/77.20	83.20/82.00/82.20	83.60/86.40/84.20	81.67/81.53/81.20	100.00/100.00/100.00	80.60/81.40/81.80	85.20/84.80/83.20	76.00/77.80/76.20	80.60/81.33/80.40
MIM+IBTA	100.00/100.00/100.00	80.40/82.40/81.20	86.60/85.20/86.80	86.80/89.60/89.60	84.60/85.73/85.80	100.00/100.00/100.00	84.00/84.80/84.40	87.00/87.20/86.80	79.40/80.40/81.80	83.47/84.13/84.30
TIM	100.00/100.00/100.00	95.80/97.60/98.80	99.00/100.00/100.00	98.80/99.80/100.00	97.87/99.13/99.60	100.00/100.00/100.00	94.20/95.60/96.60	95.60/96.20/97.40	92.60/93.80/96.00	94.13/95.20/96.67
TIM+IBTA	100.00/100.00/100.00	98.00/98.60/99.80	99.40/100.00/100.00	99.60/99.33/99.93	99.00/99.33/99.93	100.00/100.00/100.00	95.20/95.60/97.60	96.60/97.80/98.20	85.00/95.20/96.80	95.60/96.20/97.53
DIM	100.00/100.00/100.00	96.60/97.20/98.60	98.60/99.20/99.60	99.20/99.40/100.00	98.13/98.60/99.40	100.00/100.00/100.00	95.60/96.60/96.00	96.60/97.60/98.20	93.40/95.40/96.60	95.20/96.53/96.93
DIM+IBTA	100.00/100.00/100.00	97.40/98.60/99.20	99.00/99.60/99.80	99.40/100.00/100.00	98.60/99.40/99.67	100.00/100.00/100.00	95.60/97.00/97.20	97.00/97.60/98.80	94.40/95.80/97.40	95.67/96.80/97.80

Attack	Src:VGG19bn (untargeted)					Src:Res152 (untargeted)				
	→VGG19bn*	→Res50	→Dense121	→Res152	AVG Transfer Rate	→Res152*	→VGG19bn	→Res50	→Dense121	AVG Transfer Rate
MIM	100.00/100.00/100.00	58.80/57.80/56.60	62.20/60.80/60.00	45.60/44.40/44.00	55.53/54.33/53.53	100.00/100.00/100.00	73.00/73.20/73.20	88.60/89.20/89.40	79.80/79.60/82.20	80.47/80.66/81.60
MIM+IBTA	100.00/100.00/100.00	63.00/63.40/62.60	66.00/68.20/66.40	49.20/48.40/49.40	59.40/60.00/59.47	100.00/100.00/100.00	75.40/76.20/75.60	90.60/91.40/91.80	84.60/85.00/83.20	83.53/84.20/83.53
TIM	100.00/100.00/100.00	84.00/87.80/89.60	88.80/91.20/98.60	74.20/77.40/79.80	82.33/85.47/89.83	100.00/100.00/100.00	92.80/93.80/94.40	97.60/99.00/99.20	98.40/98.60/98.60	96.27/97.13/97.40
TIM+IBTA	100.00/100.00/100.00	86.60/90.60/93.20	92.80/93.00/98.60	79.20/83.40/84.60	86.20/89.00/92.13	100.00/100.00/100.00	93.80/95.80/96.80	98.20/99.40/99.80	98.40/99.20/99.20	96.80/98.13/98.60
DIM	100.00/100.00/100.00	81.80/84.40/86.20	84.80/87.80/90.80	67.00/70.80/74.60	77.87/81.00/83.87	100.00/100.00/100.00	90.60/95.20/95.60	97.60/99.20/99.40	97.20/98.60/98.20	95.13/97.67/97.73
DIM+IBTA	100.00/100.00/100.00	85.40/89.40/90.80	88.60/92.00/93.40	74.00/75.40/79.60	82.67/85.60/87.33	100.00/100.00/100.00	94.00/95.80/96.40	99.40/99.60/99.60	98.20/99.00/99.00	97.20/98.13/98.33

Attack	Src:Res50 (targeted)					Src:Dense121 (targeted)				
	→Res50*	→VGG19bn	→Dense121	→Res152	AVG Transfer Rate	→Dense121*	→VGG19bn	→Res50	→Dense121	AVG Transfer Rate
MIM	100.00/100.00/100.00	1.56/0.96/0.73	3.29/2.38/2.29	3.58/3.24/3.00	2.81/2.19/2.01	100.00/100.00/100.00	1.73/1.33/0.93	2.42/1.69/1.58	1.67/1.29/1.04	1.94/1.44/1.18
MIM+IBTA	100.00/100.00/100.00	1.96/1.60/1.51	3.96/3.40/3.18	4.20/4.02/3.93	3.37/3.01/2.87	100.00/100.00/100.00	2.53/1.98/1.58	3.38/2.87/2.76	1.87/1.98/1.71	2.59/2.28/2.02
TIM	99.89/100.00/100.00	13.24/18.36/19.02	26.78/38.64/43.91	25.11/36.33/42.13	21.71/31.10/35.02	100.00/100.00/100.00	8.64/10.87/10.53	13.91/16.87/19.62	8.76/11.62/12.98	10.44/13.12/14.38
TIM+IBTA	99.96/100.00/100.00	14.51/21.71/23.09	28.91/45.71/48.76	26.51/43.13/47.73	23.31/36.85/39.86	100.00/100.00/100.00	9.84/12.60/13.22	15.29/20.69/23.64	10.78/14.51/16.47	11.97/15.93/17.78
DIM	99.96/100.00/100.00	13.62/17.64/19.96	25.36/36.53/42.78	22.80/32.47/37.76	20.59/28.88/33.50	100.00/100.00/100.00	10.07/11.53/11.80	14.98/17.56/19.53	9.09/11.18/12.29	11.38/13.42/14.54
DIM+IBTA	100.00/100.00/100.00	14.24/22.62/23.76	25.89/42.71/46.31	23.76/39.51/45.09	21.30/34.95/38.39	100.00/100.00/100.00	11.80/14.60/14.98	15.93/22.47/25.00	10.91/14.76/16.89	12.88/17.28/18.96

Attack	Src:VGG19bn (targeted)					Src:Res152 (targeted)				
	→VGG19bn*	→Res50	→Dense121	→Res152	AVG Transfer Rate	→Res152*	→VGG19bn	→Res50	→Dense121	AVG Transfer Rate
MIM	100.00/100.00/100.00	0.60/0.40/0.40	0.62/0.29/0.29	0.33/0.20/0.20	0.52/0.30/0.30	100.00/100.00/100.00	1.16/0.93/1.02	5.93/5.07/5.00	3.36/2.42/2.36	3.48/2.81/2.79
MIM+IBTA	100.00/100.00/100.00	0.64/0.56/0.53	0.73/0.44/0.40	0.40/0.40/0.29	0.59/0.47/0.41	100.00/100.00/100.00	1.60/1.56/1.04	7.22/7.73/6.89	4.38/3.53/3.38	4.40/4.27/3.77
TIM	100.00/100.00/100.00	3.67/2.73/2.89	4.51/3.62/3.67	2.02/1.41/1.53	3.40/2.60/2.70	99.73/100.00/100.00	10.09/12.44/13.22	27.20/39.13/44.18	21.73/29.73/33.89	19.67/27.10/30.43
TIM+IBTA	100.00/100.00/100.00	5.29/4.44/5.07	6.87/6.27/6.18	2.44/2.53/2.31	4.87/4.41/4.52	99.91/100.00/100.00	10.22/14.40/15.49	27.89/45.04/51.00	23.87/36.53/41.62	20.66/31.99/36.04
DIM	99.91/100.00/100.00	3.16/2.16/2.56	4.40/3.16/3.13	1.53/0.96/1.20	3.03/2.09/2.30	99.58/100.00/100.00	9.00/11.24/14.00	25.82/37.91/44.24	20.38/29.51/34.47	18.40/26.22/30.90
DIM+IBTA	100.00/100.00/100.00	4.16/3.87/3.60	5.60/5.11/5.27	1.93/1.67/1.62	3.90/3.55/3.50	99.87/100.00/100.00	10.42/14.98/16.42	26.71/44.84/49.56	22.38/35.78/40.40	19.83/31.87/35.46

TABLE II

TRANSFER SUCCESS RATE (%) FOR NON-TARGETED ATTACKS.

Attack	Src:Inc-v3						
	→Inc-v3*	→Inc-v4	→IncRes-v2	→Adv-Inc-v3	IncRes-v2ens	ViT	AVG
MIM	100.00	49.00	42.20	38.40	21.00	38.60	37.84
DIM	100.00	70.20	63.80	45.00	25.80	39.20	48.80
SI-NIM	99.80	44.20	37.80	37.00	22.00	38.20	35.84
ATTA	100.00	72.60	65.00	45.80	26.60	39.60	49.92
VMI-CTM	99.60	67.20	67.20	45.60	26.00	39.60	51.56
PAM	100.00	81.40	68.60	47.20	27.80	39.80	52.96
Logits	100.00	85.60	79.60	50.80	28.80	40.20	57.00
RAP+LS	100.00	85.60	82.00	52.20	32.00	40.80	58.52
S ² I-TI-DIM	100.00	92.00	87.20	57.00	36.00	41.20	62.68
Logits+IBTA	100.00	88.60	80.00	51.40	31.20	42.40	58.72
RAP+LS+IBTA	100.00	88.60	82.00	52.40	32.20	43.20	59.68
S ² I-TI-DIM+IBTA	100.00	93.40	89.60	60.40	42.20	44.80	66.08

Attack	Src:Ensemble						
	→Ensemble*	→Inc-v4	→IncRes-v2	→Adv-Inc-v3	IncRes-v2ens	ViT	AVG
MIM	99.20	70.40	61.80	43.80	26.40	40.20	48.52
DIM	99.20	93.00	89.20	54.60	39.40	40.80	63.40
SI-NIM	98.60	70.00	60.60	42.00	26.40	39.80	47.76
ATTA	99.40	94.20	91.00	55.60	40.20	41.20	64.44
VMI-CTM	99.40	96.80	91.40	56.20	41.20	41.40	65.40
PAM	100.00	97.60	93.60	60.20	42.80	41.80	67.20
Logits	100.00	98.00	96.20	63.00	43.80	42.00	68.60
RAP+LS	100.00	98.20	98.60	63.60	44.00	42.40	70.04
S ² I-TI-DIM	99.80	99.80	99.60	73.60	60.40	42.60	75.20
Logits+IBTA	100.00	99.20	97.60	64.40	48.20	43.60	70.60
RAP+LS+IBTA	100.00	99.40	98.60	65.60	51.40	43.80	71.76
S ² I-TI-DIM+IBTA	100.00	99.40	99.60	78.80	65.40	44.80	77.60

TABLE III

TRANSFER SUCCESS RATE (%) FOR TARGETED ATTACKS.

Attack	Src:Inc-v3						
	→Inc-v3*	→Inc-v4	→IncRes-v2	→Adv-Inc-v3	IncRes-v2ens	ViT	AVG
MIM	99.32	0.40	0.36	0.16	0.09	0.21	0.24
DIM	99.13	2.11	1.36	0.18	0.11	0.33	0.82
SI-NIM	99.01	0.24	0.16	0.07	0.09	0.19	0.15
ATTA	99.16	2.36	1.62	0.16	0.18	0.37	0.94
VMI-CTM	99.23	2.82	1.58	0.20	0.13	0.32	1.01
PAM	99.45	2.97	1.71	0.24	0.22	0.43	1.11
Logits	99.81	3.56	1.96	0.16	0.16	0.46	1.26
RAP+LS	100.00	4.16	3.16	0.20	0.13	0.51	1.63
S ² I-TI-DIM	99.67	10.33	9.11	0.84	0.47	0.73	4.30
Logits+IBTA	100.00	3.69	2.80	0.27	0.20	0.61	1.51
RAP+LS+IBTA	100.00	5.56	3.53	0.22	0.27	0.65	2.05
S ² I-TI-DIM+IBTA	100.00	11.13	10.22	0.91	0.56	0.82	4.73

Attack	Src:Ensemble						
	→Ensemble*	→Inc-v4	→IncRes-v2	→Adv-Inc-v3	IncRes-v2ens	ViT	AVG
MIM	98.57	1.78	1.11	0.16	0.13	0.26	0.69
DIM	98.02	13.29	9.24	0.22	0.33	0.38	4.69
SI-NIM	97.68	1.87	1.04	0.09	0.09	0.22	0.66
ATTA	98.96	14.82	11.02	0.18	0.16	0.49	5.33
VMI-CTM	98.82	18.32	16.68	0.39	0.47	0.45	7.26
PAM	99.13	22.45	19.27	0.46	0.53	0.51	8.64
Logits	99.78	37.84	26.71	0.67	0.67	0.73	13.32
RAP+LS	100.00	46.07	31.27	0.62	0.60	0.77	17.87
S ² I-TI-DIM	99.01	41.22	36.56	2.96	3.00	1.85	17.12
Logits+IBTA	99.82	40.87	30.42	0.73	0.98	0.88	14.76
RAP+LS+IBTA	100.00	49.29	35.96	0.93	0.98	1.02	17.64
S ² I-TI-DIM+IBTA	99.26	42.67	37.98	3.28	3.36	2.25	17.91

References

- [1] Christian Szegedy, Wojciech Zaremba, Ilya Sutskever, Joan Bruna, Dumitru Erhan, Ian Goodfellow, and Rob Fergus. Intriguing properties of neural networks. *arXiv preprint arXiv:1312.6199*, 2013.
- [2] Ian J Goodfellow, Jonathon Shlens, and Christian Szegedy. Explaining and harnessing adversarial examples. *arXiv preprint arXiv:1412.6572*, 2014.
- [3] Yanpei Liu, Xinyun Chen, Chang Liu, and Dawn Song. Delving into transferable adversarial examples and black-box attacks. In *International Conference on Learning Representations*, 2016.
- [4] Biqing Qi, Bowen Zhou, Weinan Zhang, Jianxing Liu, and Ligang Wu. Improving robustness of intent detection under adversarial attacks: A geometric constraint perspective. *IEEE Trans. Neural Networks Learn. Syst.*, 35(5):6133–6144, 2024.
- [5] Junqi Gao, Biqing Qi, Yao Li, Zhichang Guo, Dong Li, Yuming Xing, and Dazhi Zhang. Perturbation towards easy samples improves targeted adversarial transferability. In *Advances in Neural Information Processing Systems*, 2023.
- [6] Nicholas Carlini and David Wagner. Towards evaluating the robustness of neural networks. In *2017 IEEE Symposium on Security and Privacy (SP)*, pages 39–57. Ieee, 2017.
- [7] Aleksander Madry, Aleksandar Makelov, Ludwig Schmidt, Dimitris Tsipras, and Adrian Vladu. Towards deep learning models resistant to adversarial attacks. In *International Conference on Learning Representations*, 2018.
- [8] Yinpeng Dong, Fangzhou Liao, Tianyu Pang, Hang Su, Jun Zhu, Xiaolin Hu, and Jianguo Li. Boosting adversarial attacks with momentum. In *Proceedings of the IEEE conference on computer vision and pattern recognition*, pages 9185–9193, 2018.
- [9] Jiadong Lin, Chuanbiao Song, Kun He, Liwei Wang, and John E Hopcroft. Nesterov accelerated gradient and scale invariance for adversarial attacks. In *International Conference on Learning Representations*, 2019.
- [10] Yinpeng Dong, Tianyu Pang, Hang Su, and Jun Zhu. Evading defenses to transferable adversarial examples by translation-invariant attacks. In *Proceedings of the IEEE/CVF Conference on Computer Vision and Pattern Recognition*, pages 4312–4321, 2019.
- [11] Junhua Zou, Zhisong Pan, Junyang Qiu, Xin Liu, Ting Rui, and Wei Li. Improving the transferability of adversarial examples with resized-diverse-inputs, diversity-ensemble and region fitting. In *European Conference on Computer Vision*, pages 563–579. Springer, 2020.
- [12] Xiaosen Wang, Xuanran He, Jingdong Wang, and Kun He. Admix: Enhancing the transferability of adversarial attacks. In *Proceedings of the IEEE/CVF International Conference on Computer Vision*, pages 16158–16167, 2021.
- [13] Maosen Li, Cheng Deng, Tengjiao Li, Junchi Yan, Xinbo Gao, and Heng Huang. Towards transferable targeted attack. In *Proceedings of the IEEE/CVF Conference on Computer Vision and Pattern Recognition*, pages 641–649, 2020.
- [14] Zhengyu Zhao, Zhuoran Liu, and Martha Larson. On success and simplicity: A second look at transferable targeted attacks. *Advances in Neural Information Processing Systems*, 34:6115–6128, 2021.
- [15] Muzammal Naseer, Salman Khan, Munawar Hayat, Fahad Shahbaz Khan, and Fatih Porikli. On generating transferable targeted perturbations. In *Proceedings of the IEEE/CVF International Conference on Computer Vision*, pages 7708–7717, 2021.
- [16] Zhipeng Wei, Jingjing Chen, Zuxuan Wu, and Yu-Gang Jiang. Enhancing the self-universality for transferable targeted attacks. In *Proceedings of the IEEE/CVF Conference on Computer Vision and Pattern Recognition*, pages 12281–12290, 2023.
- [17] Junyoung Byun, Seungju Cho, Myung-Joon Kwon, Hee-Seon Kim, and Changick Kim. Improving the transferability of targeted adversarial examples through object-based diverse input. In *Proceedings of the IEEE/CVF Conference on Computer Vision and Pattern Recognition*, pages 15244–15253, 2022.
- [18] Naftali Tishby, Fernando C Pereira, and William Bialek. The information bottleneck method. *arXiv preprint physics/0004057*, 2000.
- [19] Naftali Tishby and Noga Zaslavsky. Deep learning and the information bottleneck principle. In *2015 IEEE information theory workshop (itw)*, pages 1–5. IEEE, 2015.
- [20] Alexander A Alemi, Ian Fischer, Joshua V Dillon, and Kevin Murphy. Deep variational information bottleneck. In *International Conference on Learning Representations*, 2016.
- [21] Martin J Wainwright, Michael I Jordan, et al. Graphical models, exponential families, and variational inference. *Foundations and Trends® in Machine Learning*, 1(1–2):1–305, 2008.
- [22] Mohamed Ishmael Belghazi, Aristide Baratin, Sai Rajeshwar, Sherjil Ozair, Yoshua Bengio, Aaron Courville, and Devon Hjelm. Mutual information neural estimation. In *International conference on machine learning*, pages 531–540. PMLR, 2018.
- [23] Jia Deng, Wei Dong, Richard Socher, Li-Jia Li, Kai Li, and Li Fei-Fei. Imagenet: A large-scale hierarchical image database. In *2009 IEEE conference on computer vision and pattern recognition*, pages 248–255. Ieee, 2009.
- [24] Kaiming He, Xiangyu Zhang, Shaoqing Ren, and Jian Sun. Deep residual learning for image recognition. In *Proceedings of the IEEE conference on computer vision and pattern recognition*, pages 770–778, 2016.
- [25] Gao Huang, Zhuang Liu, Laurens Van Der Maaten, and Kilian Q Weinberger. Densely connected convolutional networks. In *Proceedings of the IEEE conference on computer vision and pattern recognition*, pages 4700–4708, 2017.
- [26] Karen Simonyan and Andrew Zisserman. Very deep convolutional networks for large-scale image recognition. *arXiv preprint arXiv:1409.1556*, 2014.
- [27] Zeyu Qin, Yanbo Fan, Yi Liu, Li Shen, Yong Zhang, Jue Wang, and Baoyuan Wu. Boosting the transferability of adversarial attacks with reverse adversarial perturbation. *Advances in Neural Information Processing Systems*, 35:29845–29858, 2022.
- [28] Christian Szegedy, Vincent Vanhoucke, Sergey Ioffe, Jon Shlens, and Zbigniew Wojna. Rethinking the inception architecture for computer vision. In *Proceedings of the IEEE conference on computer vision and pattern recognition*, pages 2818–2826, 2016.
- [29] Christian Szegedy, Sergey Ioffe, Vincent Vanhoucke, and Alexander Alemi. Inception-v4, inception-resnet and the impact of residual connections on learning. In *Proceedings of the AAAI conference on artificial intelligence*, volume 31, 2017.
- [30] Alexey Dosovitskiy, Lucas Beyer, Alexander Kolesnikov, Dirk Weissenborn, Xiaohua Zhai, Thomas Unterthiner, Mostafa Dehghani, Matthias Minderer, Georg Heigold, Sylvain Gelly, Jakob Uszkoreit, and Neil Houlsby. An image is worth 16x16 words: Transformers for image recognition at scale. In *9th International Conference on Learning Representations, ICLR 2021, Virtual Event, Austria, May 3-7, 2021*. OpenReview.net, 2021.
- [31] Weibin Wu, Yuxin Su, Michael R. Lyu, and Irwin King. Improving the transferability of adversarial samples with adversarial transformations. In *IEEE Conference on Computer Vision and Pattern Recognition, CVPR 2021, virtual, June 19-25, 2021*, pages 9024–9033. Computer Vision Foundation / IEEE, 2021.
- [32] Xiaosen Wang and Kun He. Enhancing the transferability of adversarial attacks through variance tuning. In *IEEE Conference on Computer Vision and Pattern Recognition, CVPR 2021, virtual, June 19-25, 2021*, pages 1924–1933. Computer Vision Foundation / IEEE, 2021.
- [33] Jianping Zhang, Jen-tse Huang, Wenxuan Wang, Yichen Li, Weibin Wu, Xiaosen Wang, Yuxin Su, and Michael R. Lyu. Improving the transferability of adversarial samples by path-augmented method. In *IEEE/CVF Conference on Computer Vision and Pattern Recognition, CVPR 2023, Vancouver, BC, Canada, June 17-24, 2023*, pages 8173–8182. IEEE, 2023.
- [34] Yuyang Long, Qilong Zhang, Boheng Zeng, Lianli Gao, Xianglong Liu, Jian Zhang, and Jingkuan Song. Frequency domain model augmentation for adversarial attack. In *European Conference on Computer Vision*, pages 549–566. Springer, 2022.